Langmuir

Article

pubs.acs.org/Langmuir

A Theoretical Analysis of Colloid Attachment and Straining in Chemically Heterogeneous Porous Media

Scott A. Bradford,*[,†] Saeed Torkzaban,[‡] and Alexander Shapiro[§]

[†]US Salinity Laboratory, USDA, ARS, Riverside, California 92507, United States

[‡]CSIRO Land and Water, Glen Osmond, SA 5064, Australia

[§]Center for Energy Resources Engineering, Department of Chemical and Biochemical Engineering, Technical University of Denmark, Lyngby, Denmark

ABSTRACT: A balance of applied hydrodynamic (T_H) and resisting adhesive (T_A) torques was conducted over a chemically heterogeneous porous medium that contained random roughness of height h_r to determine the fraction of the solid surface area that contributes to colloid immobilization (S_f*) under unfavorable attachment conditions. This model considers resistance due to deformation and the horizontal component of the adhesive force (F_{AT}), spatial variations in the pore scale velocity distribution, and the influence of h_r on lever arms for T_H and T_A. Values of S_f* were calculated for a wide range of physicochemical properties to gain insight into mechanisms and factors influencing colloid immobilization. Colloid attachment processes were demonstrated to depend on solution ionic strength (IS), the colloid radius (r_c), the Young's modulus (K), the amount of chemical heterogeneity (P_+), and the Darcy velocity (q). Colloid immobilization was also demonstrated to occur on a rough surface in the absence of attachment. In this case, S_f* depended on IS, r_c, the roughness fraction (f_0), h_r, and q. Roughness tended to enhance T_A and diminish T_H. Consequently, the effect of IS on S_f* was enhanced by h_r relative to attachment. In contrast, the effects of r_c and q on S_f* were diminished by h_r in comparison to attachment. Colloid immobilization adjacent to macroscopic roughness locations shares many similarities to grain−grain contact points and may be viewed as a type of straining process. In general, attachment was more important for higher IS and variance in the secondary minimum, and for smaller r_c, q, and K, but diffusion decreased these values. Conversely, straining was dominant for the opposite conditions. Discrepancies in the literature on mechanisms of colloid retention are likely due to a lack of consideration of all of these factors.

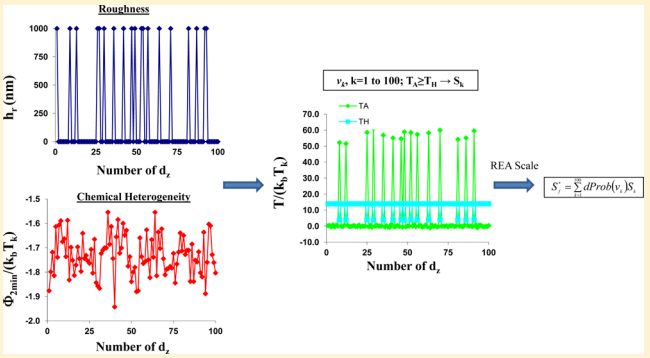

INTRODUCTION

An understanding of and ability to predict conditions that influence colloid immobilization and release are needed for numerous environmental and industrial applications. Colloid retention and release are well-known to depend on the solution and solid phase chemistry conditions[1−5] and on the system hydrodynamics.[6−9] Rolling has been demonstrated to be the dominant hydrodynamic mechanism of colloid removal from the solid−water interface (SWI) under laminar flow conditions.[6,7,10,11] Consequently, a balance of applied hydrodynamic (T_H, M L^2 T^{-2}, where M, L, and T denote units of mass, length, and time, respectively) and resisting adhesive (T_A, M L^2 T^{-2}) torques can be used to determine criteria for colloid immobilization and release.[6,8,9,11,12] Colloids will roll over the SWI when $T_H > T_A$ and will be immobilized when $T_H \leq T_A$.

The equations to determine T_H from the pore scale water velocity distribution are well-known and accepted.[12−14] In contrast, the proper formulation for forces and torques associated with adhesive interactions are much less certain, especially for conditions unfavorable for colloid attachment.[15,16] Derjaguin−Landau−Verwey−Overbeek (DLVO) theory is commonly used to estimate the adhesive force that acts perpendicular to the SWI (F_{AP}; M L T^{-2}) from electrostatic and van der Waals forces.[17,18] A tangential component of the adhesive force (F_{AT}; M L T^{-2}) also occurs in the presence of nanoscale physical and/or chemical heterogeneity[19−24] that will produce a corresponding value of T_A.

Methods to characterize the influence of physical and/or chemical heterogeneity on T_A have not yet been fully resolved at the interface scale, let alone the representative elementary area (REA) scale. Johnson, Kendall, and Roberts (JKR) theory[25] has been employed to determine T_A due to deformation.[8,26−28] Other researchers have used an empirical frictional force (F_F, M L T^{-2}) that acts tangential to the SWI to create T_A.[6,12] In contrast, some have neglected T_A altogether and implicitly assumed that colloid immobilization only occurs in the primary minimum.[29,30] However, this approach does not allow for colloid immobilization in a secondary minimum in the

Received: March 26, 2013
Revised: May 9, 2013
Published: May 20, 2013

presence of water flow which contradicts many experimental observations.[4,16]

As mentioned above, torque balance calculations can be used to determine colloid immobilization and rolling at a particular location. The value of T_H is spatially distributed in a porous medium because of differences in the pore scale velocity distribution. Bradford et al.[11] calculated and developed predictive procedures to determine the log-normal cumulative density function (CDF) of T_H on well-defined sphere packs for various average water velocities, grain sizes, and colloid sizes. These authors evaluated the CDF for T_H at a given value of T_A to determine the fraction of the porous medium surface (S_f*) that may contribute to colloid immobilization. Bradford and Torkzaban[31] further extended this approach to the case of a chemically heterogeneous porous media. Previous attempts to determine S_f* have employed JKR theory to determine T_A based on resistance due to deformation[28,31] and neglected the potential contribution of F_{AT} on T_A. Furthermore, this analysis applied to colloid attachment in a primary and/or secondary minimum on a smooth SWI and neglected the potential influence of larger scale roughness and grain−grain contacts on colloid retention. Consequently, predicted values of S_f* were likely underestimated.

The pore space geometry is known to influence the determination of T_A and T_H.[32−34] In particular, larger scale roughness has been demonstrated to enhance T_A and reduce T_H.[32,33] Consequently, higher values of S_f* are expected on a collector with large scale roughness than on a smooth collector. Indeed, enhanced colloid retention has been microscopically observed to occur near larger scale roughness locations[35−37] and at grain−grain contact points.[38,39] Colloid retention at larger scale surface roughness locations and grain−grain contacts share many similarities, including low velocity regions, multiple SWI interfaces, and different lever arms for T_A and T_H than on smooth surfaces.[40] Consequently, colloid retention at locations of larger scale roughness and grain−grain contacts may be viewed as a type of straining process (e.g., preferential retention occurring in the smallest regions of the pore space near multiple SWIs).[40] Consistent with this terminology, Tufenkji et al.[41] indicated that straining behavior was strongly dependent on the roughness properties of the sand.

Theoretically sound procedures are needed to determine colloid immobilization and release in porous medium under various solution chemistry and hydrodynamic conditions. Accurate determination of the parameter S_f* is therefore critically important. For example, S_f* may be used in continuum scale transport models to determine the maximum solid phase concentration of retained colloids,[42] to estimate the effects of velocity on the colloid sticking efficiency (α),[9] and to determine the rate of colloid immobilization.[28] Furthermore, release of colloids due to transient solution chemistry and hydrodynamic conditions can be directly related to changes in S_f*.[43,44] The objective of this work is to develop improved approaches to predict T_A in chemically heterogeneous porous media and then use this information to determine meaningful estimates of S_f* under saturated conditions. The effects of chemical heterogeneity, larger scale roughness, solution ionic strength (IS), and colloid size on S_f* were subsequently investigated and used to improve our understanding of colloid attachment and straining processes.

TORQUE BALANCE

Our torque balance considers forces and torques that act on a colloid adjacent to the SWI as a result of fluid flow and adhesive interactions. Relevant forces, lever arms, and torques are illustrated in Figure 1 for a deforming colloid adjacent to a homogeneous SWI (Figure 1a), a nondeforming colloid adjacent to a chemically heterogeneous SWI (Figure 1b), and a deforming colloid adjacent to a homogeneous SWI and a roughness of height h_r [L] (Figure 1c). The pore scale water velocity distribution creates a lift force that acts on the colloid perpendicular to the SWI and a drag force (F_D, M L T^{-2}) that acts on the colloid tangential to the SWI. The lift force is negligible when the flow is laminar.[45] Conversely, F_D is significant and it produces T_H. It should be mentioned that we have assumed that the colloid is neutrally buoyant, so that gravity can be neglected. Colloid diffusion will be discussed at the end of the next section.

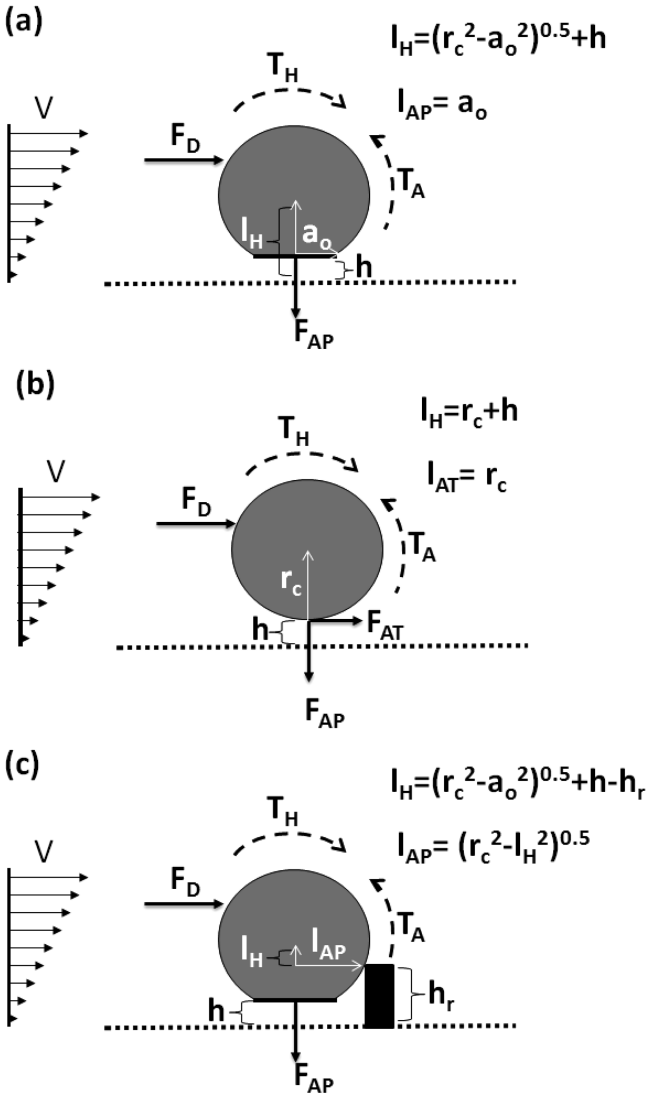

Figure 1. Relevant forces, lever arms, and torques for a deforming colloid adjacent to a homogeneous SWI (a), a nondeforming colloid adjacent to a chemically heterogeneous SWI (b), and a deforming colloid adjacent to a homogeneous SWI and a roughness of height h_r (c).

dx.doi.org/10.1021/la4011357 | Langmuir 2013, 29, 6944−6952

The value of F_D at a separation distance (h, L) shown in Figure 1 is given as[12−14]

$$F_D = 6\pi\mu_w\tau_w r_c(r_c + h)C_h \quad (1)$$

where r_c [L] is the colloid radius, τ_w [T^{-1}] is the hydrodynamic shear, μ_w [M $L^{-1}T^{-1}$] is the water viscosity, and C_h is a dimensionless function that depends on h as[12]

$$C_h = \frac{1.7007337 + 1.0221616(h/r_c)}{1 + 1.0458291(h/r_c) - 0.0014884708(h/r_c)^2} \quad (2)$$

The value of T_H for a given h is[33]

$$T_H = l_H F_D + M_E \quad (3)$$

where M_E [M L^2 T^{-2}] is the external moment of surface stresses and l_H [L] is the lever arm associated with F_D. The value of M_E is given as[12]

$$M_E = 4\pi\mu_w\tau_w r_c^3 C_{2h} \quad (4)$$

where C_{2h} is a second dimensionless function that depends on h as[12]

$$C_{2h} = 0.054651334[18.276952 - \exp(-1.422943(h/r_c))] \quad (5)$$

The value of l_H (Figure 1) is given as[33]

$$l_H = \sqrt{r_c^2 - a_0^2} + h - h_r \quad (6)$$

where is a_0 [L] is the contact radius. When $h_r > (r_c^2 - a_0^2)^{1/2} + h$, the value of $l_H = 0$ because the rolling point occurs at a height of $(r_c^2 - a_0^2)^{1/2} + h$. The determination of a_0 will be discussed shortly.

The value of F_{AP} shown in Figure 1 is required to mobilize a colloid from a secondary minimum in the interaction energy, Φ_{2min} [ML^2T^{-2}], and it can be calculated as[46,47]

$$F_{AP} = \max\left(\frac{\partial\Phi_{2min}}{\partial h}\right) \quad (7)$$

Here "max" denotes the maximum value of the derivative in the interaction energy adjacent to Φ_{2min}. Similarly, a value of F_{AT} on a heterogeneous surface may be determined as[19]

$$F_{AT} = \frac{\partial\Phi_{2min}}{\partial z} \quad (8)$$

where z [L] is the distance in the tangential direction on the SWI.

JKR theory can be used to estimate a_0 (found in eq 6) due to particle deformation that arises from F_{AP}. When the colloid is in adhesive contact with the surface, the value of a_0 is given as[25]

$$a_0 = \left(\frac{4F_{AP}r_c}{K}\right)^{1/3} \quad (9)$$

where K [M L^{-1} T^{-2}] is the composite Young's modulus. Conversely, at separation (assumed in this work) this value of a_0 is multiplied by 0.63.[26] It should be mentioned that other approaches may also be employed to determine a_0.[48,49]

A value of T_A arising from both F_{AP} and F_{AT} is given as

$$T_A = l_{AP}F_{AP} + l_{AT}F_{AT} \quad (10)$$

where l_{AP} [L] and l_{AT} [L] are the lever arms associated with F_{AP} and F_{AT}, respectively. When $h_r > h$, the values of l_{AP}[33] and l_{AT} are given as

$$l_{AP} = \sqrt{r_c^2 - l_H^2} \quad (11)$$

$$l_{AT} = \sqrt{r_c^2 - a_0^2} \quad (12)$$

When $h_r \le h$, then $l_{AP} = a_0$, whereas l_{AT} is still given by eq 12. In the absence of nanoscale physical and chemical heterogeneity, the second term on the right-hand side of eq 10 is zero. Conversely, in the absence of deformation and large scale roughness the first term on the right side of eq 10 is zero.

COLLOID IMMOBILIZATION AT THE REA SCALE

Values of the mean and standard deviation for the secondary minimum at the REA scale (Φ_{2min}*) in a chemically heterogeneous porous medium were determined.[31,50] In brief, only a portion of the SWI contributes to the colloid−SWI interaction energy at any particular location.[12] This area of electrostatic influence (A_z, L^2) was discretized into a number of equally sized cells to represent the smallest sized chemical heterogeneity of interest. Each cell was associated with a zeta potential (ζ_- or ζ_+) and a cross-sectional area of A_h (L^2). Mean values of Φ_{2min} were calculated for possible charge realizations within A_z using a linear combination of interaction energies from cells with ζ_- and ζ_+.[51] The interaction energies considered electrostatics,[52] retarded London−van der Waals attraction,[53] and Born repulsion[54] and assumed a sphere−plate geometry. The probability of a given charge realization in A_z was calculated using a binomial mass distribution, assuming that the heterogeneity was randomly distributed and that the total fraction of cells with ζ_+ was known at the REA scale (P_+). The probability density function (PDF) for Φ_{2min}* on the chemically heterogeneous surface was subsequently calculated and used to determine mean and standard deviations for Φ_{2min}*. Simulation values were in excellent agreement with Monte Carlo simulation output using computationally intensive grid surface integration techniques.

In this work, the SWI was discretized into segments of length d_z [L], where d_z is the diameter of A_z. Mean values and standard deviations for Φ_{2min}* on the chemically heterogeneous surface were calculated as described above and then used to randomly generate Φ_{2min} on the SWI with these same statistical properties (see the graphical abstract). Binary values of h_r (equal to 0 or h_r) were also randomly assigned to each segment, so that the total fraction of segments with $h_r = 0$ and h_r were equal to the selected probabilities of $(1 - f_0)$ and f_0, respectively. It should be mentioned that the value of h_r does not influence Φ_{2min} when the cross-sectional area of h_r is equal to A_z.[50]

Values of F_{AP} and F_{AT} at a particular location i were approximated as

$$F_{AP}^i \cong \frac{\Phi_{2min}^i}{h_{2min}^*} \quad (13)$$

$$F_{AT}^i \cong \frac{\Phi_{2min}^i - \Phi_{2min}^{i+1}}{d_z} \quad (14)$$

where the superscripts i and $i + 1$ are used to denote adjacent spatial A_z locations, and h_{2min}^* [L] is the separation distance associated with Φ_{2min}*. Equation 13 is based on approximations from Derjaguin and Langbein.[55] Simulation results demonstrated that this approximation was consistent with values determined using eq 7 (data not shown). Equation 14 follows directly from eq 8. The value of T_A is given as (eq 10)

dx.doi.org/10.1021/la4011357 | Langmuir 2013, 29, 6944−6952

$$T_A^i = l_{AP}^i F_{AP}^i + l_{AT}^i F_{AT}^i \quad (15)$$

Here the values of l_{AP}^i and l_{AT}^i are functions of Φ_{2min}^i (eq 9). In addition, the value of l_{AP}^i is also a function of h_r (eq 6), but it only applies at a location i ($h_r = 0$) when location $i + 1$ has h_r.

The pore scale velocity distribution adjacent to the SWI of a porous medium can be quantified using a log-normal CDF.[11] The corresponding probability of obtaining a velocity (v), dProb(v), that acts on a colloid of given radius adjacent to the SWI is given as

$$\mathrm{dProb}(v) = \frac{1}{v\sigma\sqrt{2\pi}} \exp\left(-\frac{(\ln[v] - \ln[v_{50}])^2}{2\sigma^2}\right) \mathrm{d}v \quad (16)$$

where v_{50} [M L^2 T^{-2}] and σ [−] are the median and variance of the log-normal distribution of velocity adjacent to the SWI, respectively. Bradford et al.[11] presented a method to predict the CDF of v for various colloid radii, Darcy velocities, and collector grain sizes based on the solution of Stokes and continuity equations in sphere packs using scaling procedures. In the current work, the PDF of v was discretized into a number of categories (k = 1−100), denoted as v_k. Values of T_H were calculated (eq 3) for each location on the SWI for all v_k categories (denoted as T_H^{ik}). It is very computationally expensive to try to explicitly determine separate values of v_k near each h_r. Consequently, values of v_k near areas containing h_r have been assumed to be the same as on the smooth SWI, and the influence of h_r was implicitly included in T_H by l_H (eq 6).[33] This assumption is expected to provide a high estimate of v_k and T_H near h_r and therefore a conservative prediction of colloid retention at this location.

A torque balance was calculated for each T_A^i and T_H^{ik} on the SWI. Positive values of T_A^i act in the opposite direction as T_H^{ik} to decelerate and/or to immobilize colloids ($T_H^{ik} \leq T_A^i$) when water flow is in the direction of increasing z. Conversely, negative values of T_A^i act in the same direction to T_H^{ik} to promote rolling ($T_H^{ik} > T_A^i$). The fraction of the SWI that contributes to colloid immobilization ($S_k = n_f/(n_f + n_{uf})$, where n_f and n_{uf} are the number of segments that were favorable and unfavorable for colloid immobilization) was determined for each v_k based on the torque balance. The total value of S_f* at the REA scale was calculated as

$$S_f^* = \sum_{k=1}^{100} \mathrm{dProb}(v_k) S_k \quad (17)$$

The kinetic energy of a diffusing colloid produces a Brownian force and torque that acts in a random direction and with a variable magnitude over time. The torque arising from the Brownian force was therefore not explicitly considered in our torque balance to determine S_f*. However, the Maxwellian kinetic energy model for diffusing colloids[31,56,57] has been used to estimate α as a function of Φ_{2min}* as

$$\alpha = \mathrm{erf}\left(\sqrt{\varphi_{2min}^*}\right) - \sqrt{\frac{4\varphi_{2min}^*}{\pi}} \exp\left(-\varphi_{2min}^*\right) \quad (18)$$

Here $\varphi_{2min}^* = \Phi_{2min}^*/(k_b T_k)$, where k_b is the Boltzmann constant and T_k is the absolute temperature. This approach considers the relative strengths of the Brownian kinetic energy and the interaction energy for colloids to determine α but neglects the observed influence of hydrodynamic forces on experimental values of α.[9,58] Some researchers have attempted to account for this velocity dependency by multiplying α by S_f*.[9,43] This same approach (multiplying α by S_f*) may also be viewed as a way to correct S_f* for diffusion.

RESULTS AND DISCUSSION

Below we present calculated values of S_f* for various IS (1, 5, 10, 25, 50, 75, and 100 mM) and r_c (50, 250, 500, 1250, and 2500 nm) under unfavorable attachment conditions. The parameter values of K, P_+, F_{AT}, Darcy velocity (q), and h_r were selected to study colloid attachment and straining processes. For these calculations the Hamaker constant equaled 5×10^{-21} J, the characteristic wavelength was 100 nm, the collision diameter was 0.5 nm, A_h = 50 nm^2, ζ_+ = 50 mV, ζ_- = −70 mV, the colloid zeta potential equaled −27 mV, and the median sand grain size was 360 μm.

Colloid Attachment. Previous research has largely neglected the contribution of F_{AT} and h_r on colloid immobilization. In this case, colloid immobilization in the presence of fluid flow may occur as a result of deformation. Deformation of the colloid and/or SWI may occur in the presence of water flow because of F_{AP}.[10] Figure 2 presents simulated values of S_f* on a chemically heterogeneous SWI (P_+ = 0.25) for various r_c and IS when only deformation (F_{AT} = 0 and h_r = 0) was considered in the torque balance calculations. Three values of K were considered in these simulations, namely, 4.014E8 (Figure 2a), 4.014E9 (Figure 2b), and 4.014E10 N m^{-2} (Figure 2c). For a given r_c the value of S_f* tended to increase with IS due to an increase in Φ_{2min}* and F_{AP}. Conversely, for a given IS the value of S_f* decreased with r_c, in spite of the larger value of Φ_{2min}*. The value of T_H increases with the cube of r_c when h = 0 (eq 1). Consequently, T_H increases more rapidly than T_A with r_c, and the value of S_f* therefore rapidly decreased with increasing r_c. Similar trends for S_f* with r_c were obtained from fitted values to colloid breakthrough curves in column studies and earlier torque balance calculations.[8,31,43] Figure 2 also demonstrates that S_f* is a strong function of K that increases with decreasing K. This result has important implications for colloid transport, retention, and release. In particular, this observation indicates that more rigid colloids will experience less retention than flexible colloids (such as bacteria) even if they have identical interaction energies. In support of this finding, the hydrodynamic threshold was lower to remove similarly sized glass than polystyrene particles from a glass surface in parallel flow chamber experiments.[10]

A colloid may also be immobilized in the presence of fluid flow due to the contribution of F_{AT} (nanoscale heterogeneity) on T_A, even in the absence of deformation (a_0 = 0) and roughness (h_r = 0). Figure 3 presents similar information as in Figure 2 when P_+ = 0.05 (Figure 3a), 0.1 (Figure 3b), and 0.25 (Figure 3c). Other simulation parameters were the same as in Figure 2. Colloid immobilization increased with P_+. The value of S_f*also exhibited a similar dependency on IS and r_c as in Figure 2. However, the magnitude of S_f* tended to be lower for smaller r_c when considering F_{AT} than for only deformation. In the presence of nanoscale chemical heterogeneity the value of S_f*increases with the variance in Φ_{2min}* for a given IS and r_c. Results from Bradford and Torkzaban[31,50] indicate that this variance increases with A_h and with the difference in magnitude between ζ_+ and ζ_-. In addition, the height and amount of nanoscale roughness will also influence the variance in Φ_{2min}*,[50] but these effects were not considered in Figure 3. Consequently, the relative importance of F_{AT} to deformation on

dx.doi.org/10.1021/la4011357 | Langmuir 2013, 29, 6944−6952

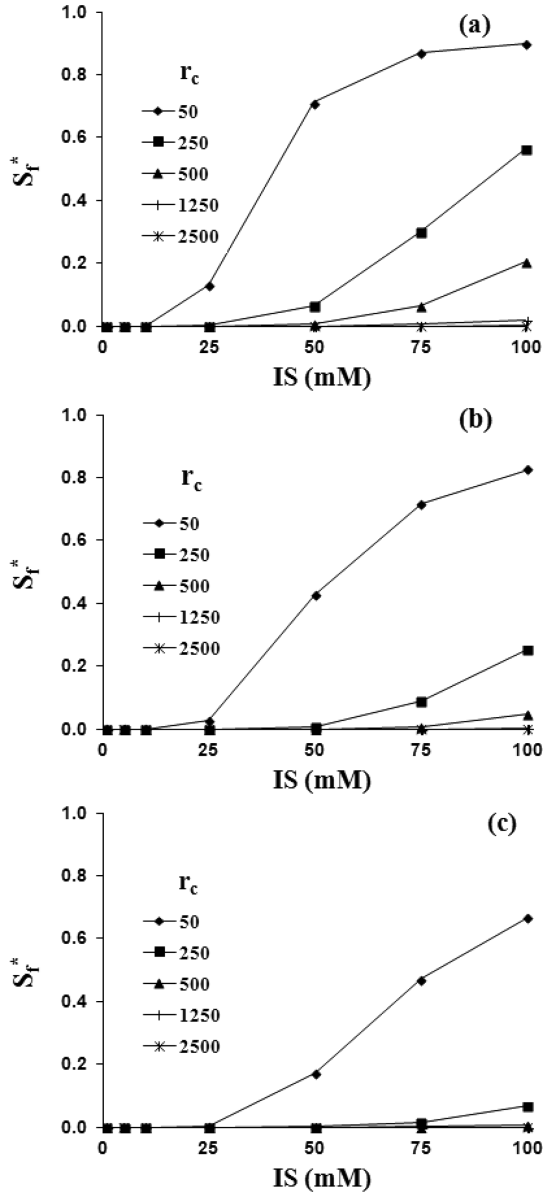

Figure 2. Simulated values of S_f^* for various r_c and IS conditions when only deformation was considered in the torque balance. Three values of the K were considered in these simulations, namely, 4.014E8 (a), 4.014E9 (b), and 4.014E10 N m^{-2} (c). Other simulation parameters are listed in the text.

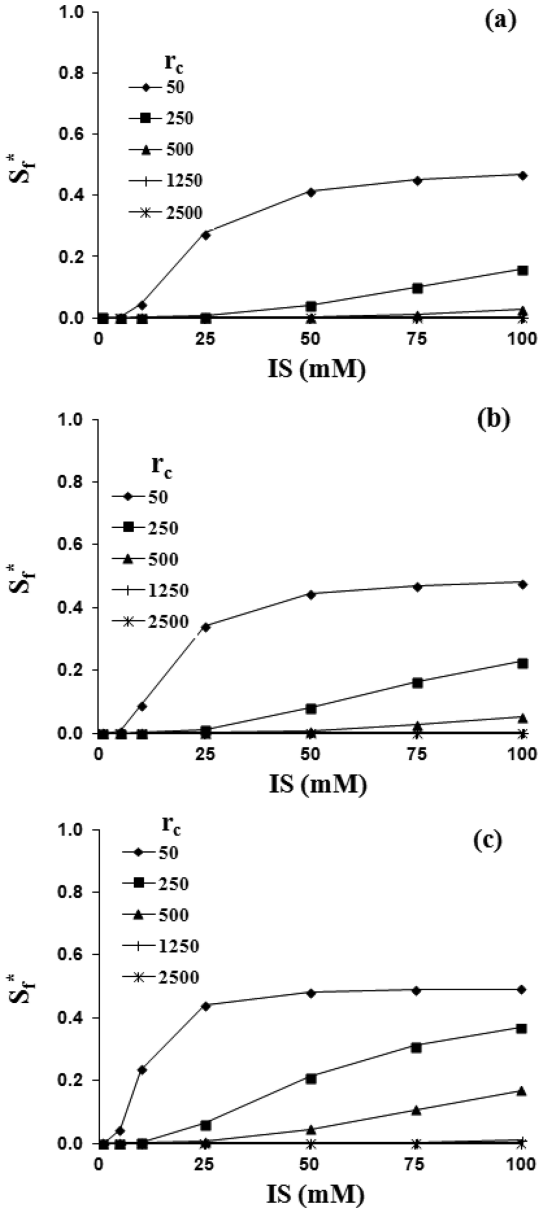

Figure 3. Simulated values of S_f^* for various r_c and IS conditions when only F_{AT} was considered in the torque balance. Three values of the P_+ were considered in these simulations, namely, 0.05 (a), 0.1 (b), and 0.25 (c). Other simulation parameters are listed in the text.

colloid immobilization will depend on both nanoscale chemical and physical heterogeneity parameters.

Figure 4a presents simulated values of S_f^* for the various r_c and IS when both deformation ($a_0 > 0$) and nanoscale chemical heterogeneity ($F_{AT} > 0$) are considered in the torque balance calculations, but in the absence of roughness ($h_r = 0$). Values of K = 4.014E9 N m^{-2} and P_+ = 0.25 were selected for these simulations. Other model parameters were the same as in Figures 2 and 3. Simulation results were nearly identical to that shown in Figure 3c, suggesting that colloid immobilization was dominated by the variance in Φ_{2min} which determined F_{AT}. Furthermore, note that values of S_f^* in Figure 4a were actually sometimes lower than when only deformation occurred (Figure 2b). This is because positive and negative values of F_{AT} may occur, and the negative values of F_{AT} diminished the influence of deformation on colloid immobilization. However, it should be recognized that deformation is likely to play a more significant role in determining S_f^* for lower values of K (Figure 2) and P_+ (Figure 3).

Figures 4b and 4c present similar information to Figure 4a, but for different values of q. In the case of Figures 4a, 4b, and 4c values of q were equal to 0.1, 1, and 0.01 cm min^{-1}, respectively. These values of q were selected to encompass a range in water velocities found in coarse textured porous media. Velocity was observed to have a large impact on values of S_f^* when r_c is large but had a minor influence on S_f^* for smaller r_c because of the dependence of T_H on the cube of r_c.[8] Velocity effects were more significant at higher IS because values of S_f^* were also larger.

Roughness and Colloid Straining. The above analyses considered smooth surfaces and neglected the effects of larger scale surface roughness and grain−grain contacts on colloid

dx.doi.org/10.1021/la4011357 | Langmuir 2013, 29, 6944−6952

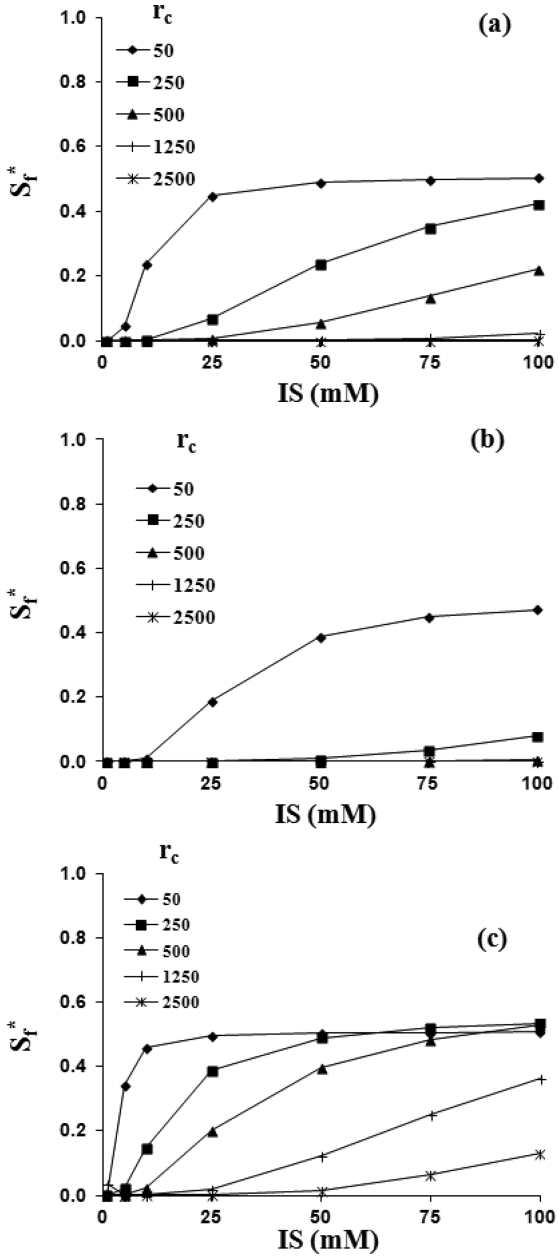

Figure 4. Simulated values of S_f^* for various r_c and IS conditions when both deformation (K = 4.014E9 N m^{-2}) and F_{AT} (P_+ = 0.25) were considered in the torque balance. Three values of q were considered in these simulations, namely, 0.1 (a), 1.0 (b), and 0.01 cm min^{-1} (c). Other simulation parameters are listed in the text.

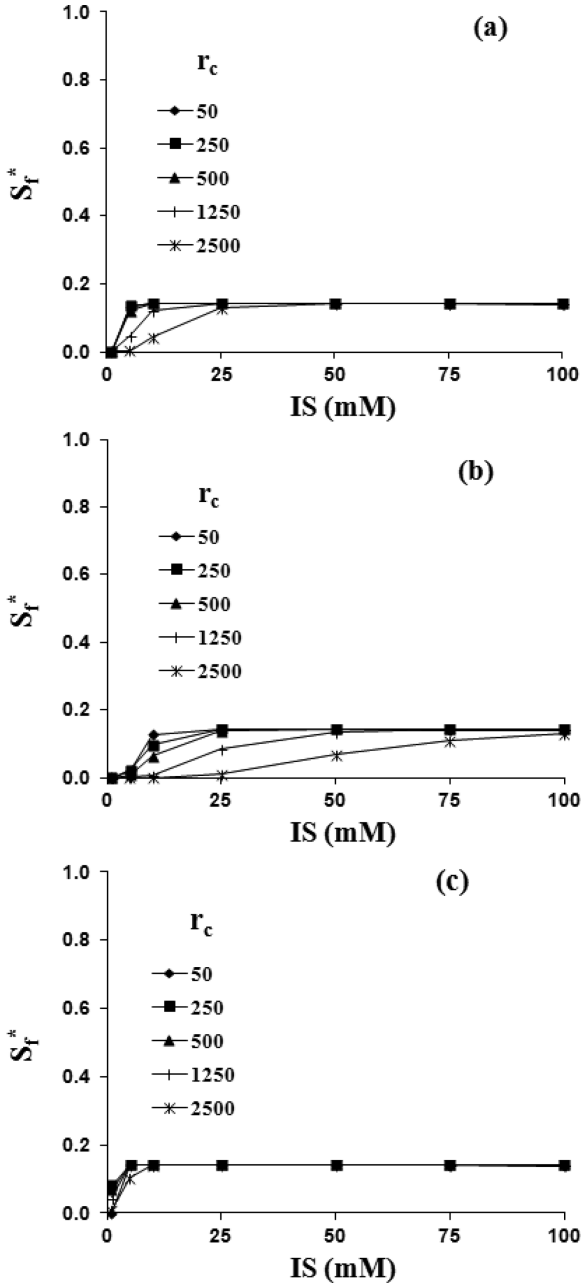

Figure 5. Simulated values of S_f^* for various r_c and IS conditions when only h_r = 1000 nm (f_0 = 0.2) was considered in the torque balance. Three values of q were considered in these simulations, namely, 0.1 (a), 1.0 (b), and 0.01 cm min^{-1} (c). Other simulation parameters are listed in the text.

immobilization. Figure 5a presents simulated values of S_f^* on a rough surface (f_o = 0.2 and h_r = 1000 nm) for various r_c and IS when both deformation (a_o = 0) and nanoscale chemical heterogeneity (F_{AT} = 0) were neglected in the torque balance calculations. Other model parameters were the same as in Figure 4a. It should be emphasized that no colloid attachment occurred in Figure 5 in the absence of roughness. Consequently, all values of S_f^* were strictly due to the presence of h_r.

Roughness influences the lever arms that act on T_A and T_H (Figure 1). The value of T_A tends to be enhanced adjacent to roughness, whereas T_H is diminished. Both of these factors will lead to greater retention adjacent to roughness locations than on flat surfaces. Similar to Figures 2–4, the value of S_f^* increased with IS and decreased with r_c. However, the functional dependence of S_f^*on IS and r_c was different than for attachment (Figures 2–4) because of the difference in the lever arms. All values of S_f^* approach a threshold with increasing IS that was determined by f_0. Increasing h_r produces a more rapid rise to this threshold value of S_f^*, especially for smaller r_c (data not shown), because l_H increases with $r_c + h - h_r$ (eq 6).

Figures 5b and 5c present similar information to Figure 5a, but for different values of q. In the case of Figures 5a, 5b, and 5c values of q were equal to 0.1, 1, and 0.01 cm min^{-1}, respectively. Similar to Figure 4, larger colloids were more susceptible to the influence of velocity than smaller colloids.

dx.doi.org/10.1021/la4011357 | *Langmuir* 2013, 29, 6944–6952

However, velocity had a much smaller influence on values of S_f* than for the case of only attachment (Figure 4). The value of S_f* for larger colloids was therefore larger on rough (Figure 5) than smooth surfaces (Figure 4). Note that l_H and l_{AP} go to zero and r_c, respectively, as h_r approaches $r_c + h$ (eqs 6 and 11). Consequently, roughness provides an increasing shield against the effects of velocity as h_r increases (eqs 3 and 6) and T_A dramatically increases (see the graphical abstract).

Values of S_f* were greater on rough (Figure 5a) than on smooth (Figure 4a) surfaces when r_c > 500 nm. Consequently, roughness had a much more significant influence on colloid immobilization than attachment for these larger colloids. Similarly, straining processes have been observed to play a dominant role in colloid retention for larger colloids under unfavorable attachment conditions.[38,59] A similar torque balance procedure (eq 18) may be applied to represent grain−grain contact points and larger scale surface roughness locations because $T_H = 0$ and $l_{AP} = r_c$ when $h_r > r_c + h$.[32] Colloid immobilization is always favorable when $T_H = 0$, regardless of Φ_{2min}*. The number of grain−grain contact points within a REV is expected to increase with a decrease in grain size. Consequently, the value of f_0 and S_f* are also expected to increase with a decrease in grain size. These trends are consistent with experimental observations.[59]

It should be mentioned that the relative importance of attachment to straining on colloid immobilization will depend on the velocity and the solution chemistry (Figures 4 and 5). Straining tends to becomes more important for higher r_c and q and for smaller IS, grain sizes, and variances in Φ_{2min}*. Attachment will be more important for the opposite conditions. Consequently, some of the discrepancies reported in the literature[60] concerning mechanisms of colloid retention are likely to be due to a lack of consideration of all of these factors.

Colloid Attachment and Straining. Figure 6a presents simulated values of S_f* on a rough surface (with $f_0 = 0.2$ and h_r = 1000 nm) for various r_c and IS when deformation ($a_0 > 0$) and nanoscale chemical heterogeneity ($F_{AT} > 0$) were also considered in the torque balance calculations. Other model parameters were the same as in Figure 5a. The simulation results tended to be a superposition of the behavior observed in Figures 4a and 5a. Values of S_f* again increased with IS and decreased with r_c. Similar to behavior shown in Figure 5a, the values of S_f* were greater in Figure 6a than those shown in Figure 4a when r_c > 500 nm as a result of roughness. In contrast, the values of S_f* in Figure 6a were greater than those shown in Figure 5a when r_c < 500 nm because of attachment (Figure 4a). Consequently, straining processes dominated the retention of larger colloids, whereas retention of smaller colloids was controlled by attachment. However, the relative importance of these factors will also depend on K, IS, r_c, chemical heterogeneity, q, grain size, and f_0 as indicated above.

It should be emphasized that the amount of colloid retention in a particular location will depend on the rate of mass transfer to and from locations defined by S_f*. Colloid filtration theory has been developed to determine the rate of colloid mass transfer from the bulk aqueous phase to the SWI.[61] One potential way to account for the influence of diffusion on S_f* is to multiply S_f* by α (eq 18). Figure 6b presents values of αS_f* for various IS and r_c when the simulation conditions were the same as in Figure 6a. Similar to Figure 6a, the values of αS_f* increase with IS. In contrast, values of αS_f* (Figure 6b) were smaller than S_f* (Figure 6a), especially for smaller IS and r_c, and the maximum value of αS_f* occurred for the intermediate r_c

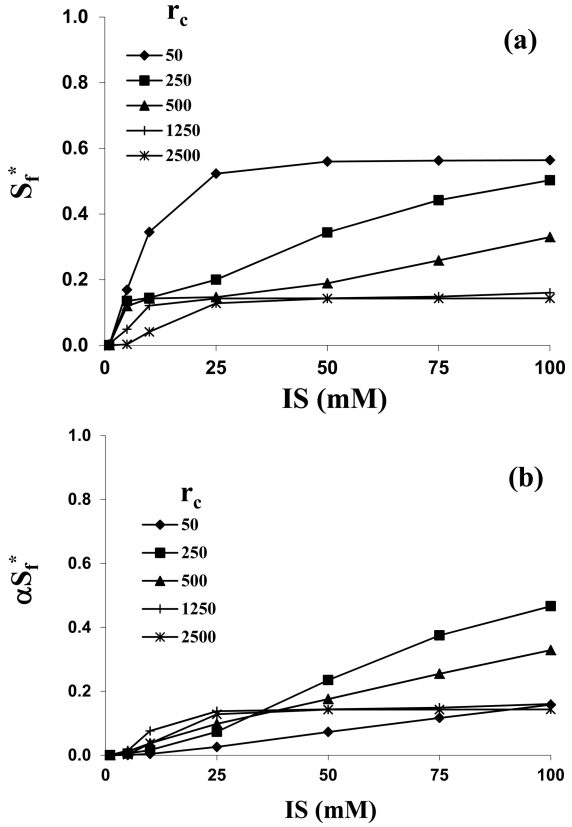

Figure 6. Simulated values of S_f* (a) and αS_f* (b) for various r_c and IS conditions when deformation (K = 4.014E9 N m^{-2}), F_{AT} (P_+ = 0.25), and h_r = 1000 nm (f_0 = 0.2) were considered in the torque balance. The value of q was 0.1 cm min^{-1}. Other simulation parameters are listed in the text.

= 250 nm. Consequently, diffusion will tend to increase the relative importance of straining to attachment. In addition to diffusion, solid phase mass transfer from unfavorable ($1 - S_f$*) to favorable (S_f*) locations may occur by rolling under the influence of hydrodynamic forces.[28] Additional research and modeling techniques (trajectory analysis) are needed to fully resolve these mass transfer issues.

CONCLUSIONS

A mechanistic description of T_H and T_A is provided for chemically heterogeneous porous media. The value of T_A depends on the resistance due to deformation and F_{AT}. The model also considers the effects of spatial variations in the pore scale velocity distribution that occurs in a porous media on T_H. In addition, the model accounts for variations in the lever arms that occur near randomly generated larger scale surface roughness features. A torque balance was conducted over the heterogeneous porous medium surface to determine S_f*. Values of S_f* were calculated for a wide range of properties (IS, r_c, K, P_+, q, and h_r) under unfavorable attachment conditions to gain insight into mechanisms and factors influencing colloid immobilization.

Results demonstrate a complex coupling between many factors influencing colloid immobilization. Colloid attachment processes (h_r = 0) were demonstrated to depend on IS, r_c, K, P_+, and q. Greater values of S_f* due to attachment occurred for higher IS and P_+ and for lower values of r_c, K, and q. The value of F_{AT}, due to the variance in Φ_{2min}*, mainly determined S_f*

dx.doi.org/10.1021/la4011357 | Langmuir 2013, 29, 6944−6952

when K was high (deformation is less significant). This variance in Φ_{2min}* depends on nanoscale chemical and/or physical heterogeneity parameters.

Colloid immobilization was also demonstrated to occur on a rough surface in the absence of attachment. In this case, S_f* depended on IS, r_c, f_o, h_r, and q. Values of S_f* approached a threshold value determined by f_0 at higher IS. Higher values of S_f* occurred with larger h_r and smaller r_c and q. Roughness tended to enhance T_A and diminish T_H. Consequently, the effect of IS on S_f* was enhanced relative to attachment. In contrast, the effects of r_c and q on S_f* were diminished by h_r in comparison to attachment. Colloid immobilization adjacent to macroscopic roughness locations shares many similarities to grain−grain contact points because it involves retention at multiple SWI interfaces and similar modifications to lever arms. Furthermore, colloid immobilization can occur at both of these locations in the absence of attachment. Consequently, colloid immobilization at larger surface roughness locations may be viewed as a type of straining process.[40]

The relative importance of attachment and straining processes will depend on a wide range in parameters. In general, attachment is more important for higher IS and variance in Φ_{2min}* and for smaller r_c, q, and K. Conversely, straining at larger roughness locations and grain−grain contacts will be more important for the opposite conditions. Accounting for diffusion on S_f* with αS_f* tends to decrease the relative importance of attachment to straining, especially for smaller IS and r_c. Discrepancies in the literature on mechanisms of colloid retention are likely due a lack of consideration of all of these factors.

AUTHOR INFORMATION

Corresponding Author

*Phone 951-369-4857; e-mail Scott.Bradford@ars.usda.gov (S.A.B.).

Notes

The authors declare no competing financial interest.

ACKNOWLEDGMENTS

This research was supported by the USDA, ARS, NP 214. The USDA is an equal opportunity provider and employer.

REFERENCES

(1) Lenhart, J. J.; Saiers, J. E. Colloid mobilization in water-saturated porous media under transient chemical conditions. *Environ. Sci. Technol.* **2003**, *37*, 2780−2787.

(2) Shiratori, K.; Yamashita, Y.; Adachi, Y. Deposition and subsequent release of Na-kaolinite particles by adjusting pH in the column packed with Toyoura sand. *Colloids Surf., A* **2007**, *306*, 137−141.

(3) Tosco, T.; Tiraferri, A.; Sethi, R. Ionic strength dependent transport of microparticles in saturated porous media: Modeling mobilization and immobilization phenomena under transient chemical conditions. *Environ. Sci. Technol.* **2009**, *43*, 4425−4431.

(4) Torkzaban, S.; Kim, H. N.; Simunek, J.; Bradford, S. A. Hysteresis of colloid retention and release in saturated porous media during transients in solution chemistry. *Environ. Sci. Technol.* **2010**, *44*, 1662−1669.

(5) Bradford, S. A.; Kim, H. Implications of cation exchange on clay release and colloid-facilitated transport in porous media. *J. Environ. Qual.* **2010**, *39*, 2040−2046.

(6) Bergendahl, J.; Grasso, D. Colloid generation during batch leaching tests: mechanics of disaggregation. *Colloids Surf., A* **1998**, *135*, 193−205.

(7) Bergendahl, J.; Grasso, D. Prediction of colloid detachment in a model porous media: Thermodynamics. *AIChE J.* **1999**, *45*, 475−484.

(8) Torkzaban, S.; Bradford, S. A.; Walker, S. L. Resolving the coupled effects of hydrodynamics and DLVO forces on colloid attachment to porous media. *Langmuir* **2007**, *23*, 9652−9660.

(9) Shen, C.; Huang, Y.; Li, B.; Jin, Y. Predicting attachment efficiency of colloid deposition under unfavorable attachment conditions. *Water Resour. Res.* **2010**, *46*, W11526.

(10) Das, S. K.; Schechter, R. S.; Sharma, M. M. The role of surface roughness and contact deformation on the hydrodynamic detachment of particles from surfaces. *J. Colloid Interface Sci.* **1994**, *164*, 63−77.

(11) Bradford, S. A.; Torkzaban, S.; Wiegmann, A. Pore scale simulations to determine the applied hydrodynamic torque and colloid immobilization. *Vadose Zone J.* **2011**, *10*, 252−261.

(12) Duffadar, R. D.; Davis, J. M. Dynamic adhesion behavior of micrometer scale particles flowing over patchy surfaces with nanoscale electrostatic heterogeneity. *J. Colloid Interface Sci.* **2008**, *326*, 18−27.

(13) Goldman, A. J.; Cox, R. G.; Brenner, H. Slow viscous motion of a sphere parallel to a plane wall - I motion through a quiescent fluid. *Chem. Eng. Sci.* **1967**, *22*, 637−651.

(14) O'Neill, M. E. A sphere in contact with a plane wall in a slow linear shear flow. *Chem. Eng. Sci.* **1968**, *23*, 1293−1298.

(15) Johnson, W. P.; Li, X.; Tong, M.; Ma, H. Comment on "Transport and fate of bacteria in porous media: Coupled effects of chemical conditions and pore space geometry" by Saeed Torkzaban et al. *Water Resour. Res.* **2009**, *45*, W09603.

(16) Torkzaban, S.; Walker, S. L.; Bradford, S. A. Reply to comment by William P. Johnson et al. on "Transport and fate of bacteria in porous media: Coupled effects of chemical conditions and pore space geometry". *Water Resour. Res.* **2009**, *45*, W09604.

(17) Derjaguin, B. V.; Landau, L. D. Theory of the stability of strongly charged lyophobic sols and of the adhesion of strongly charged particles in solutions of electrolytes. *Acta Physicochim. U.S.S.R.* **1941**, *14*, 733−762.

(18) Verwey, E. J. W.; Overbeek, J. Th. G. *Theory of the Stability of Lyophobic Colloids*; Elsevier: Amsterdam, 1948.

(19) Czarnecki, J.; Warszynski, P. The evaluation of tangential forces due to surface inhomogeneties in the particle deposition process. *Colloids Surf.* **1987**, *22*, 207−214.

(20) Kostoglou, M.; Karabelas, A. J. Effect of roughness on energy of repulsion between colloidal surfaces. *J. Colloid Interface Sci.* **1995**, *171*, 187−199.

(21) Busscher, H. J.; Poortinga, A. T.; Bos, R. Lateral and perpendicular interaction forces involved in mobile and immobile adhesion of microorganisms on model solid surfaces. *Curr. Microbiol.* **1998**, *37*, 319−323.

(22) Velegol, D.; Catana, S.; Anderson, J. L.; Garoff, S. Tangential forces between nontouching colloidal particles. *Phys. Rev. Lett.* **1999**, *83*, 1243−1246.

(23) Anderson, J. L.; Velegol, D.; Garoff, S. Measuring colloidal forces using differential electrophoresis. *Langmuir* **2000**, *16*, 3372−3384.

(24) Shen, C.; Wang, F.; Li, B.; Jin, Y.; Wang, L.-P.; Huang, Y. Application of DLVO energy map to evaluate interactions between spherical colloids and rough surfaces. *Langmuir* **2012**, *28*, 14681−14692.

(25) Johnson, K. L.; Kendall, K.; Roberts, A. D. Surface energy and the contact of elastic solids. *Proc. R. Soc. London, Ser. A* **1971**, *324*, 301−313.

(26) Bergendahl, J.; Grasso, D. Prediction of colloid detachment in a model porous media: hydrodynamics. *Chem. Eng. Sci.* **2000**, *55*, 1523−1532.

(27) Bradford, S. A.; Torkzaban, S.; Walker, S. L. Coupling of physical and chemical mechanisms of colloid straining in saturated porous media. *Water Res.* **2007**, *41*, 3012−3024.

(28) Bradford, S. A.; Torkzaban, S.; Simunek, J. Modeling colloid transport and retention in saturated porous media under unfavorable attachment conditions. *Water Resour. Res.* **2011**, *47*, W10503.

(29) Yang, C.; Dabros, T.; Li, D.; Czarnecki, J.; Masliyah, J. H. Kinetics of particle transport to a solid surface from an impinging jet under surface and external force fields. *J. Colloid Interface Sci.* **1998**, *208*, 226−240.
(30) Johnson, W. P.; Li, X. Q.; Yal, G. Colloid retention in porous media: Mechanistic confirmation of wedging and retention in zones of flow stagnation. *Environ. Sci. Technol.* **2007**, *41*, 1279−1287.
(31) Bradford, S. A.; Torkzaban, S. Colloid adhesive parameters for chemically heterogeneous porous media. *Langmuir* **2012**, *28*, 13643−13651.
(32) Vaidyanathan, R.; Tien, C. Hydrosol deposition in granular media under unfavorable surface conditions. *Chem. Eng. Sci.* **1991**, *46*, 967−983.
(33) Burdick, G. M.; Berman, N. S.; Beaudoin, S. P. Hydrodynamic particle removal from surfaces. *Thin Solid Films* **2005**, *488*, 116−123.
(34) Shen, C.; Huang, Y.; Li, B.; Jin, Y. Effects of solution chemistry on straining of colloids in porous media under unfavorable conditions. *Water Resour. Res.* **2008**, *44*, W05419.
(35) Choi, N.-C.; Kim, D.-J.; Kim, S.-B. Quantification of bacterial mass recovery as a function of pore-water velocity and ionic strength. *Res. Microbiol.* **2007**, *158*, 70−78.
(36) Wang, D. J.; Paradelo, M.; Bradford, S. A.; Peijnenburg, W.; Chu, L. Y.; Zhou, D. M. Facilitated transport of Cu with hydroxyapatite nanoparticles in saturated sand: Effects of solution ionic strength and composition. *Water Res.* **2011**, *45*, 5905−5915.
(37) Darbha, G. K.; Fischer, C.; Michler, A.; Luetzenkirchen, J.; Schäfer, T.; Heberling, F.; Schild, D. Deposition of latex colloids at rough mineral surfaces: An analogue study using nanopatterned surfaces. *Langmuir* **2012**, *28*, 6606−6617.
(38) Bradford, S. A.; Simunek, J.; Bettahar, M.; Tadassa, Y. F.; van Genuchten, M. Th.; Yates, S. R. Straining of colloids at textural interfaces. *Water Resour. Res.* **2005**, *41*, W10404.
(39) Xu, S.; Gao, B.; Saiers, J. E. Straining of colloidal particles in saturated porous media. *Water Resour. Res.* **2006**, *42*, W12S16.
(40) Bradford, S. A.; Torkzaban, S. Colloid transport and retention in unsaturated porous media: A review of interface-, collector-, and pore scale processes and models. *Vadose Zone J.* **2008**, *7*, 667−681.
(41) Tufenkji, N.; Miller, G. F.; Ryan, J. N.; Harvey, R. W.; Elimelech, M. Transport of *Cryptosporidium* oocysts in porous media: Role of straining and physicochemical filtration. *Environ. Sci. Technol.* **2004**, *38*, 5932−5938.
(42) Bradford, S. A.; Kim, H. N.; Haznedaroglu, B. Z.; Torkzaban, S.; Walker, S. L. Coupled factors influencing concentration-dependent colloid transport and retention in saturated porous media. *Environ. Sci. Technol.* **2009**, *43*, 6996−7002.
(43) Bradford, S. A.; Torkzaban, S.; Kim, H.; Simunek, J. Modeling colloid and microorganism transport and release with transients in solution ionic strength. *Water Resour. Res.* **2012**, *48*, W09509.
(44) Bedrikovetsky, P.; Siqueira, F. D.; Furtado, C. de Souza, A.L.S. Modified particle detachment model for colloidal transport in porous media. *Transp. Porous Media* **2011**, *86*, 353−383.
(45) Soltani, M.; Ahmadi, G. On particle adhesion and removal mechanics in turbulent flows. *J. Adhes. Sci. Technol.* **1994**, *8*, 763−785.
(46) Sharma, P.; Flury, M.; Zhou, J. Detachment of colloids from a solid surface by a moving air-water interface. *J. Colloid Interface Sci.* **2008**, *326*, 143−150.
(47) Shang, J.; Flury, M.; Chen, G.; Zhuang, J. Impact of flow rate, water content, and capillary forces on in situ colloid mobilization during infiltration in unsaturated sediments. *Water Resour. Res.* **2008**, *44*, W06411.
(48) Derjaguin, B. V.; Muller, V. M.; Toporov, Yu. P. Effect of contact deformations on the adhesion of particles. *J. Colloid Interface Sci.* **1975**, *53*, 314−326.
(49) Maugis, D.; Pollock, H. M. Surface forces, deformations and adherence at metal microcontacts. *Acta Metall.* **1984**, *32*, 1323−1334.
(50) Bradford, S. A.; Torkzaban, S. Colloid interaction energies for physically and chemically heterogeneous porous media. *Langmuir* **2013**, *29*, 3668−3676.
(51) Bendersky, M.; Davis, J. M. DLVO interaction of colloidal particles with topographically and chemically heterogeneous surfaces. *J. Colloid Interface Sci.* **2011**, *353*, 87−97.
(52) Hogg, R.; Healy, T. W.; Fuerstenau, D. W. Mutual coagulation of colloidal dispersions. *Trans. Faraday Soc.* **1966**, *62*, 1638−1651.
(53) Gregory, J. Approximate expression for retarded van der Waals interaction. *J. Colloid Interface Sci.* **1981**, *83*, 138−145.
(54) Ruckenstein, E.; Prieve, D. C. Adsorption and desorption of particles and their chromatographic separation. *AIChE J.* **1976**, *22*, 276−285.
(55) Israelachvili, J. N. *Intermolecular and Surface Forces*; Academic Press: San Diego, CA, 1992.
(56) Simoni, S. F.; Harms, H.; Bosma, T. N. P.; Zehnder, A. J. B. Population heterogeneity affects transport of bacteria through sand columns at low flow rates. *Environ. Sci. Technol.* **1998**, *32*, 2100−2105.
(57) Shen, C.; Li, B.; Huang, Y.; Jin, Y. Kinetics of coupled primary- and secondary-minimum deposition of colloids under unfavorable chemical conditions. *Environ. Sci. Technol.* **2007**, *41*, 6976−6982.
(58) Johnson, W. P.; Li, X.; Assemi, S. Deposition and re-entrainment dynamics of microbes and non-biological colloids during non-perturbed transport in porous media in the presence of an energy barrier to deposition. *Adv. Water Resour.* **2007**, *30*, 1432−1454.
(59) Bradford, S. A.; Simunek, J.; Bettahar, M.; van Genuchten, M. Th.; Yates, S. R. Significance of straining in colloid deposition: Evidence and implications. *Water Resour. Res.* **2006**, *42*, W12S15.
(60) Johnson, W. P.; Pazmino, E.; H., M. Direct observations of colloid retention in granular media in the presence of energy barriers, and implications for inferred mechanisms from indirect observations. *Water Res.* **2010**, *44* (4), 1158−1169.
(61) Tufenkji, N.; Elimelech, M. Correlation equation for predicting single-collector efficiency in physicochemical filtration in saturated porous media. *Environ. Sci. Technol.* **2004**, *38*, 529−536.